

Distribution of Language-Related Cntnap2 Protein in Neural Circuits Critical for Vocal Learning

Michael C. Condro¹ and Stephanie A. White^{1,2*}

¹Molecular, Cellular & Integrative Physiology Interdepartmental Program, University of California, Los Angeles, California 90095

²Department of Integrative Biology & Physiology, University of California, Los Angeles, California 90095

ABSTRACT

Variants of the contactin associated protein-like 2 (Cntnap2) gene are risk factors for language-related disorders including autism spectrum disorder, specific language impairment, and stuttering. Songbirds are useful models for study of human speech disorders due to their shared capacity for vocal learning, which relies on similar cortico-basal ganglia circuitry and genetic factors. Here we investigate Cntnap2 protein expression in the brain of the zebra finch, a songbird species in which males, but not females, learn their courtship songs. We hypothesize that Cntnap2 has overlapping functions in vocal learning species, and expect to find protein expression in song-related areas of the zebra finch brain. We further expect that the distribution of this membrane-bound protein may not completely mirror its mRNA distribution due to the distinct subcellular localization of the two molecular species. We find that

Cntnap2 protein is enriched in several song control regions relative to surrounding tissues, particularly within the adult male, but not female, robust nucleus of the arcopallium (RA), a cortical song control region analogous to human layer 5 primary motor cortex. The onset of this sexually dimorphic expression coincides with the onset of sensorimotor learning in developing males. Enrichment in male RA appears due to expression in projection neurons within the nucleus, as well as to additional expression in nerve terminals of cortical projections to RA from the lateral magnocellular nucleus of the nidopallium. Cntnap2 protein expression in zebra finch brain supports the hypothesis that this molecule affects neural connectivity critical for vocal learning across taxonomic classes. *J. Comp. Neurol.* 522:169–185, 2014.

© 2013 Wiley Periodicals, Inc.

INDEXING TERMS: autism; birdsong; Caspr2; speech; zebra finch

Language is a complex phenotype unique to humans, although facets of the behavior are shared with other species. Vocal learning, the ability to imitate or to produce novel sounds, is rare in the animal kingdom, so far found only in bats, cetaceans, elephants, pinnipeds, and songbirds. Humans are the only living primate species with this ability (Knornschild et al., 2010; Fitch, 2012; Stoeger et al., 2012). Genes underlying vocal learning and language are beginning to emerge, with a major breakthrough being the identification of Forkhead Box P2 (FOXP2) as the monogenetic locus for a human speech disorder. (Abbreviations in all capitals denote the human form of the molecule, lowercase is used for animal homologs, and italics denote nucleic acids.) FOXP2 is a transcription factor, and a mutation in its DNA binding domain leads to orofacial dyspraxia in a multigenerational pedigree known as the KE family (Lai et al., 2001). Additional FOXP2 mutations are

associated with specific language impairment (SLI) and developmental verbal dyspraxia, further strengthening the link between the gene and language ability (Graham and Fisher, 2013). As a transcription factor, FOXP2's effects on language must be mediated through its gene targets. Chromatin immunoprecipitation has revealed that contactin associated protein-like 2 (*CNTNAP2*) is a direct transcriptional target of FOXP2 (Vernes et al.,

Grant sponsors: National Institutes of Health; Grant numbers: NIH 5 T32 NS058280, NIH R21 HD065271; Grant sponsor: UCLA Eureka Scholarship; Grant sponsor: UCLA Edith Hyde Fellowship (to M.C.C.); Grant sponsor: US Army; Grant number: AR093327 (to S.A.W.).

*CORRESPONDENCE TO: Stephanie A. White, PhD, Department of Integrative Biology & Physiology, University of California, Los Angeles, 610 Charles E. Young Dr. East, Los Angeles CA 90095-7239. E-mail: sawwhite@ucla.edu

Received January 28, 2013; Revised April 11, 2013;

Accepted June 19, 2013.

DOI 10.1002/cne.23394

Published online July 1, 2013 in Wiley Online Library (wileyonlinelibrary.com)

© 2013 Wiley Periodicals, Inc.

2008). *CNTNAP2* is a particularly interesting target because it has independently been associated with a language-related disorder. Specifically, Old Order Amish children afflicted with cortical dysplasia-focal epilepsy (CDFE) harbor a deletion in *CNTNAP2*. CDFE is characterized by epilepsy, mental retardation, hyperactivity, impaired social behaviors, and language regression. A majority of affected children meet criteria for autism spectrum disorder (ASD), of which language impairment is a core deficit (Strauss et al., 2006). Within the general population, *CNTNAP2* polymorphisms are associated with language-related disorders, including increased risk for ASD (Arking et al., 2008; Li et al., 2010), delayed age of first word (Alarcón et al., 2008), SLI (Newbury et al., 2011; Peter et al., 2011; Whitehouse et al., 2011), and decreased long-range connectivity of the medial prefrontal cortex (Scott-Van Zeeland et al., 2010).

The mechanistic basis of these disorders is still unclear. The best characterized function of *Cntnap2* is to cluster voltage-gated potassium channels (VGKCs) to the juxtaparanodes of nerves (Poliak et al., 2003; Horresh et al., 2008). In the central nervous system, *Cntnap2* may also affect synaptic development (Anderson et al., 2012). Transgenic mice lacking *Cntnap2* exhibit behavioral abnormalities reminiscent of patients with CDFE, namely, epilepsy, hyperactivity, diminished social activity, repetitive behaviors, and reduced frequency of ultrasonic vocalizations when pups are separated from their dams (Peñagarikano et al., 2011). This diminished vocal behavior could be due to vocal impairment or lack of motivation as a form of reduced social activity. In either case, this aspect of the model is limited because pup isolation calls are innate. Songbirds, including zebra finches, offer an advantageous model for studying the impact of *Cntnap2* given that they are vocal learners with a well-characterized neural circuitry that underlies this ability.

Like other songbirds, zebra finches possess a distinct set of interconnected brain nuclei dedicated to vocal

learning and production termed the “song circuit” (Fig. 1). The circuit consists of two pathways: the posterior vocal pathway, required for vocal production, includes a projection from the cortical nucleus HVC (proper name; Reiner et al., 2004) to the robust nucleus of the arcopallium (RA), which in turn projects to the hypoglossal nucleus (nXIIts) that controls the avian vocal organ, the syrinx (Nottebohm et al., 1976). The anterior forebrain pathway (AFP), required for song modification (Brainard and Doupe, 2000), begins with a separate subset of HVC projections to the striatopallidal nucleus area X, which projects to the medial portion of the dorsolateral nucleus of the anterior thalamus (DLM), which then projects to the lateral magnocellular nucleus of the nidopallium (LMAN), which sends nerves terminals to RA as well as back to area X. This latter pathway is a cortical-basal ganglia-thalamo-cortical loop similar to the circuitry thought to underlie vocal learning in humans (Simonyan et al., 2012). An advantage of the zebra finch model is that vocal learning behavior and anatomy is sexually dimorphic. Females have an incomplete song circuit in which area X is not fully developed (Nottebohm et al., 1976), and RA is not innervated by HVC, causing the nucleus to shrink through apoptosis (Konishi and Akutagawa, 1985; Nixdorf-Bergweiler, 1996). Consequently, males begin to sing around 35 days (d) (Immelmann, 1969; Price, 1979), whereas females have never been observed to sing in nature. The sexually dimorphic singing behavior and the underlying song circuit anatomy make zebra finches an advantageous model for studying genes related to vocal learning including human speech.

As an initial step toward using songbirds as a model for vocal deficits associated with *Cntnap2*, Panaitof et al. (2010) described endogenous mRNA expression in the zebra finch. Remarkably, *Cntnap2* punctuates the song circuit with differential expression in song nuclei relative to their surrounding tissues. In juvenile and adult males, *Cntnap2* is enriched in two cortical song nuclei, RA and LMAN, but diminished in area X. In females, *Cntnap2* levels in RA and LMAN are equivalent

Abbreviations

AD	Dorsal arcopallium	LMAN	Lateral magnocellular nucleus of the anterior nidopallium
AFP	Anterior forebrain pathway	Meso	Mesopallium
AIV	Ventral intermediate arcopallium	Mol	Molecular cell layer of the cerebellum
Arco	Arcopallium	NeuN	Neuronal nuclei
Cntnap2	Contactin associated protein-like 2	Nido	Nidopallium
d	Days of age	nXIIts	Hypoglossal nucleus
DLM	Medial portion of the dorsolateral nucleus of the anterior thalamus	Ov	Ovoid nucleus
DMP	Dorsomedial nucleus of the posterior thalamus	Pur	Purkinje cell layer of the cerebellum
Gapdh	Glyceraldehyde 3-phosphate dehydrogenase	PV	Parvalbumin
GFP	Green fluorescent protein	RA	Robust nucleus of the arcopallium
GP	Globus pallidus	St-P	Striatopallidum
Gran	Granule cell layer of the cerebellum	VGKC	Voltage-gated potassium channel
Hyper	Hyperpallium	X	Area X
Kvβ2	Potassium channel beta subunit	ZFTMA	Zebra finch immortalized cell line
LFB	Lateral forebrain bundle		

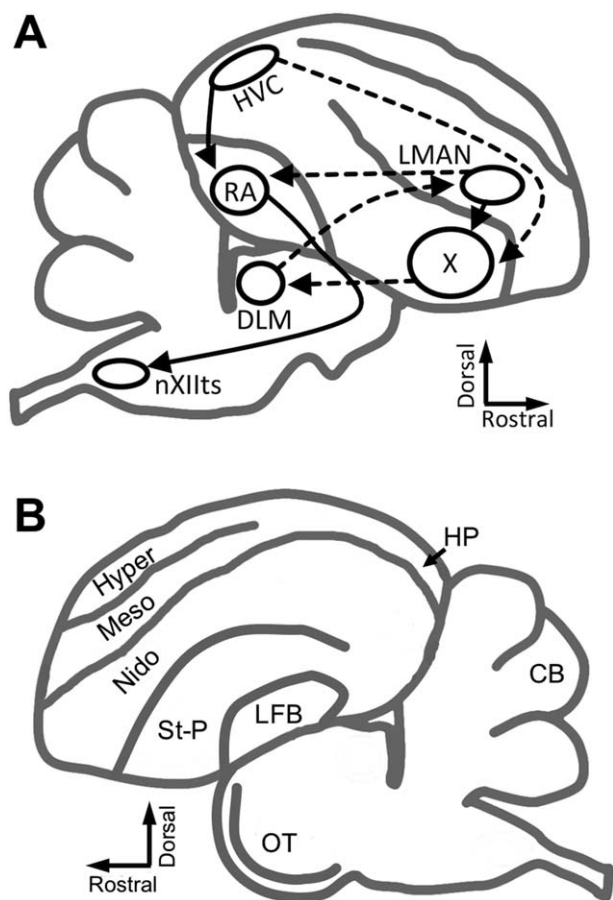


Figure 1. Diagram of the songbird brain. **A:** Schematic sagittal drawing depicts simplified song control circuitry. Solid lines indicate the posterior motor pathway, beginning with HVC, which projects to RA. RA directly projects to nXIIts, which controls the motor neurons of the syrinx. Dashed lines indicate connections of the AFP, in which HVC, X, DLM, and LMAN comprise a cortical-basal ganglia-thalamo-cortical loop like those underlying procedural learning in mammalian brains. LMAN completes the song circuit by projecting to RA, as well as back to X. **B:** Schematic sagittal drawing depicts nonsong brain regions in which *Cntnap2* immunostaining was analyzed in this study. See list for abbreviations.

to or lower than those of the surrounding arco- and nidopallium, respectively (Panaitof et al., 2010). Differential *Cntnap2* expression in the song circuit suggests that it serves a purpose in vocal learning (White, 2010; Hilliard et al., 2012). If so, translation is required for any effects on anatomy or physiology. Protein expression does not always follow that of the encoding mRNA, with a precedent in songbirds for socially regulated translation (Whitney and Johnson, 2005). We hypothesized that protein expression patterns would be largely similar to those for the mRNA, but with some differences due to posttranscriptional changes and to localization of the protein not only to cell bodies, but also along axons.

Here we validate an antibody against *Cntnap2* for use in zebra finch tissue and describe the *Cntnap2* protein distribution in the zebra finch brain at timepoints during male song development. We find that expression in song circuit neuronal cell bodies largely follows the mRNA but also highlights axonal connections critical for the vocal learning capacity. In line with this idea, within the sexually dimorphic nucleus RA, we identify projection neurons as the cell type that expresses *Cntnap2* protein.

MATERIALS AND METHODS

Animals and tissue preparation

All animal use and experimental procedures were in accordance with the National Institutes of Health (NIH) guidelines for experiments involving vertebrate animals and approved by the UCLA Chancellor's Animal Care and Use Committee. Zebra finches ($n = 32$ male and 21 female) between 25 and 500 days of age (d) used in this study were obtained from our breeding colony. Sex was determined based on sexually dimorphic plumage, or by postmortem identification of gonads at ages prior to the emergence of dimorphic plumage.

Antibody characterization

Cntnap2

In order to assess endogenous zebra finch *Cntnap2* protein levels and distribution, a commercially available anti-*Cntnap2* primary polyclonal antibody (Table 1) was selected for testing based on the perfect homology of the antigenic site (amino acids 1315–1331 in the C terminus of NCBI accession number NP_054860) between humans, rats, mice, and zebra finches. A translated nucleotide BLAST (National Center for Biotechnology Information, U.S. National Library of Medicine, Bethesda, MD) search revealed no other plausible targets in the zebra finch genome. The ability of this antibody to detect zebra finch *Cntnap2* was vetted as described below (Fig. 2).

Gapdh

Used here to measure relative levels of glyceraldehyde 3-phosphate dehydrogenase (*Gapdh*) as a loading control in western analysis, the antibody (Table 1) detects a 38-kDa band in mammalian lysates, according to the manufacturer. It has been previously used in western analysis in mice (Jones et al., 2008; Fortune and Lurie 2009) and in zebra finch (Miller et al., 2008; Hilliard et al., 2012), detecting a protein band ~ 36 kDa in the latter animal.

Potassium channel beta subunit (Kv β 2)

The Kv β 2 antibody (Table 1) was selected for use in zebra finch due to perfect homology of the antigenic

TABLE 1.
Primary Antibodies

Primary antibody	Immunogen	Manufacturer	Catalog no.	Species
Cntnap2 (Caspr2)	Synthetic peptide corresponding to amino acids 1315–1331 of rat Caspr2, accession number NP_054860)	Millipore (Temecula, CA)	AB5886	Rabbit polyclonal
Gapdh	Purified GAPDH from rabbit muscle	Millipore	MAB374	Mouse monoclonal
Kvβ2	Amino acids 17–22 of rat Kvβ2 (accession number NP_034728), conserved in zebra finch	Neuromab (Davis, CA)	K17/70	Mouse monoclonal
NeuN	Purified cell culture nuclei from mouse brain	Millipore	MAB377	Mouse monoclonal
Parvalbumin	Parvalbumin purified from carp muscles	Swant (CH)	235	Mouse monoclonal

site, amino acids 17–22 (TGSPG) of rat (accession number NP_034728), and zebra finch (NCBI RefSeq NC_011485.1). A translated nucleotide BLAST search revealed no other plausible targets of the antibody in zebra finch. Specificity of this antibody is described by the manufacturer. In western analysis, the antibody detects a major protein band at 38 kDa and a minor band at 41 kDa in brain lysates from wildtype mice, but no bands in lysates from knockout mice (http://neuromab.ucdavis.edu/datasheet/K17_70.pdf). Although the specificity of this antibody has not been confirmed for use in zebra finch, a recent study using this antibody found significant overlap of Kv1.1, Kv1.2, and Kvβ2 (Ovsepian et al., 2013), suggesting that even if the antibody is not specific to Kvβ2, it will at least have a similar immunostaining pattern. We use this antibody only to show that Cntnap2 colocalizes with potassium channel subunits and do not make any claims as to its specificity.

NeuN

The anti-NeuN antibody (Table 1) was used in this study to identify morphology in the zebra finch brain, as it was in Scott and Lois (2007). According to the manufacturer, the antibody detects protein bands at 46 and 48 kDa in western analysis.

Parvalbumin

The anti-parvalbumin antibody (Table 1) was characterized in Celio et al. (1988). It has since been used to detect the zebra finch isoform in immunohistochemistry to identify parvalbumin-positive neurons in song control nuclei (Wild et al., 2001, 2005, 2009; Roberts et al., 2007), as it is used in this study.

Cell culture

Whole brain homogenate was obtained from an adult male zebra finch. Following overdose with inhalation anesthetic (isoflurane, Phoenix Pharmaceutical, St. Joseph, MO), the brain was dissected without fixation

and homogenized with a hand-held homogenizer (Kontes, Thermo Fisher Scientific, Pittsburgh, PA) in ice-cold modified RIPA lysis buffer (pH 7.6) with protein inhibitors (No. P8340, Sigma-Aldrich, St. Louis, MO) and an RC DC Protein Assay (Bio-Rad, Hercules, CA) was performed to determine protein concentration as in Miller et al. (2008). Zebra finch ZFTMA cells (Itoh and Arnold, 2011) which do not endogenously express Cntnap2 (Fig. 2B) were transfected with either a pCR-TOPO vector (Life Technologies, Grand Island, NY) containing the complete coding sequence for zebra finch Cntnap2 (Panaitof et al., 2010) or a pGIPz vector (Thermo Scientific, Lafayette, CO) containing the GFP coding sequence only, as a negative control. Cells were transfected using a Nucleofector II and chicken nucleofector solution (Lonza, Basel, Switzerland) and distributed on BD Falcon tissue culture dishes (100 × 20 mm style, Fisher Scientific). At 24 hours posttransfection, GFP expression was observed in ~70% of cells in the plate transfected with the pGIPz vector (not shown). Forty-eight hours after transfection, cells were dissolved in ice-cold modified RIPA lysis buffer with protease inhibitors and a protein assay was performed as above.

Western analysis

Samples of both brain homogenates and cell culture lysates were prepared for immunoblotting by diluting with 2× 5% betamercaptoethanol in Laemmli buffer (pH 6.8; Bio-Rad) and storing at –80°C until use. Samples of 25 μg of brain and 100 μg of cell culture lysates were boiled for 2 minutes and then resolved on a 10% isocratic sodium dodecyl sulfate (SDS)-polyacrylamide gel in Tris-glycine-SDS buffer (pH 8.3; Bio-Rad) at 100 V. A Precision Plus Protein Dual Color Standard (Bio-Rad) was included on the gel as a molecular mass marker. Protein was then transferred onto a PVDF membrane with a pore size of 0.45 μm in Tris-glycine (Bio-Rad) with 20% methanol and 1% SDS. The membrane was blocked with 5% milk in Tris-buffered saline

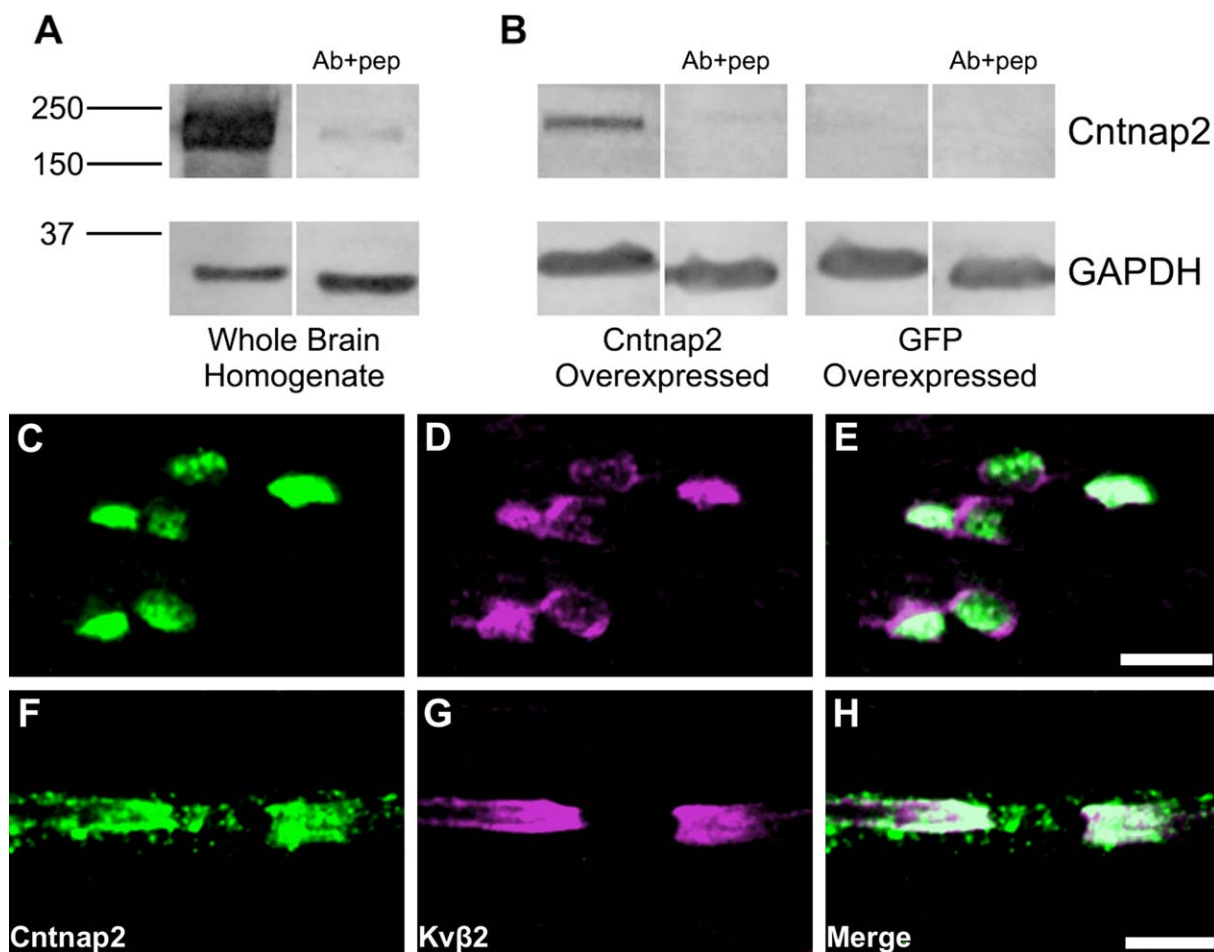


Figure 2. Antibody detection of zebra finch Cntnap2. **A:** Western blot of zebra finch whole brain homogenate. Anti-Cntnap2 primary antibody detects a single prominent protein band at the predicted molecular weight (~ 180 kDa) for endogenous zebra finch Cntnap2. **B:** Western blots of the ZFTMA zebra finch established cell line with a plasmid expressing zebra finch Cntnap2 or GFP. Transfection of the Cntnap2 construct results in a detectable signal at the predicted molecular weight for Cntnap2 (left). In contrast, transfection of GFP results in no detectable signal at the same molecular weight, confirming no endogenous Cntnap2 expression in this skin-derived cell line (right). For each condition, preadsorption of the primary antibody with its antigenic peptide (Ab+pep) dramatically reduces or removes the signal. Molecular weight markers are given in kDa. **C–E:** Zebra finch optic and **(F–H)** sciatic nerves double-labeled with Cntnap2 and potassium channel subunit Kv β 2 antibodies. Cntnap2 signal colocalizes with putative signals for potassium channel subunit Kv β 2 in both nerves, consistent with its expression in rodents (Poliak et al., 1999, 2003). Overlap of these signals in zebra finch nerves further validates the Cntnap2 antibody for use in this model. See list for abbreviations. Scale bars = 10 μ m in C–E; 5 μ m in F–H. [Color figure can be viewed in the online issue, which is available at wileyonlinelibrary.com.]

with 0.1% tween-20 (pH 7.4; TBST) for 2 hours and then incubated with the anti-Cntnap2 antibody at 1:250 and anti-Gapdh (Table 1) at 1:100,000 in 2.5% milk-TBST overnight at 4°C. A replicate set of samples was incubated with the anti-Cntnap2 antibody that had been preadsorbed with antigenic peptide (Millipore, Temecula, CA) at a ratio of 1:30 by mass. Blots were then incubated with horseradish peroxidase (HRP)-conjugated antirabbit and antimouse secondary antibodies (Table 2) at 1:2,000 and 1:10,000, respectively, in 2.5% milk-TBST for 2 hours. Blots were developed with ECL Plus, imaged on a Typhoon scanner (GE Healthcare), and signal specificity assessed.

Tissue staining and immunohistochemistry

Dissection and preparation of tissues

Birds of known age and sex were overdosed with isoflurane, then transcidentally perfused with warmed saline followed by 4% paraformaldehyde in phosphate-buffered saline (pH 7.4; PBS). Brains were dissected out and cryoprotected in a 20% sucrose solution. Forty- μ m thick sections were cut in either the coronal or sagittal orientation on a cryostat (Leica Microsystems, Bannockburn, IL) and thaw-mounted onto microscope slides (Colorfrost Plus; Fisher Scientific, Pittsburgh, PA) in a manner that produced replicate sets of adjacent or near-adjacent sections, then stored at -80°C until use.

TABLE 2.
Secondary Antibodies

Catalog no.	Manufacturer	Reactivity	Conjugate
NA931	GE Healthcare, Piscataway, NJ	Mouse IgG	Horseradish peroxidase (HRP)
NA934	GE Healthcare	Rabbit IgG	HRP
A-11008	Life Technologies, Grand Island, NY	Rabbit IgG	Alexa-Fluor 488
A-11001	Life Technologies	Mouse IgG	Alexa-Fluor 488
A-21422	Life Technologies	Mouse IgG	Alexa-Fluor 555
A-11004	Life Technologies	Mouse IgG	Alexa-Fluor 568
B-1000	Vector Laboratories, Burlingame, CA	Rabbit IgG	Biotin

Sciatic and optic nerves were dissected from two adult males following brain removal and fixed in 4% paraformaldehyde for 20 minutes, then transferred to PBS. Optic nerves were cryoprotected in a 20% sucrose solution overnight, then cryosectioned at 10 μ m thickness and mounted on microscope slides. Sciatic nerves were mechanically desheathed in PBS, teased, and dried on microscope slides.

Nerve tissue

Prior to immunostaining, sciatic nerve slides were frozen on dry ice for 5 minutes, then allowed to come back to room temperature. Slides containing nerve samples were postfixed and permeabilized in methanol at -20°C for 20 minutes. A liquid repellent border (Liquid Blocker; Ted Pella, Redding, CA) was drawn along the edges of the slide, and then the samples were rehydrated with phosphate buffer (pH 7.4; PB). Samples were blocked with 10% goat serum diluted in PB with 0.1% Triton-X and 1% glycine for 1 hour, then incubated with the anti-Cntnap2 antibody diluted to 1:500 in blocking solution overnight at 4°C . After washing with PB, samples were incubated with antirabbit Alexa Fluor 488 (Table 2) at 1:1,000 in blocking solution for 4 hours. The procedure was then repeated with anti-Kv β 2 (Table 1) at 1:250 and antimouse Alexa Fluor 568 (Table 2) at 1:1,000. Glass coverslips were mounted on slides using ProLong Gold antifade reagent (Life Technologies).

Brain sections

One of the replicate sets of brain sections from each bird was used to identify those that contained song control nuclei, using 1% thionin staining to reveal cytoarchitecture. In some cases, sections were alternatively incubated with NeuroTrace fluorescent Nissl stain (Life Technologies) diluted at 1:200 in 0.1 M PB for 20 minutes. For quantification of Cntnap2-positive neurons in RA, slides were chosen with those sections that contained the largest cross-sectional area of RA, in order to control for position within the nucleus, and thawed to room temperature. A liquid repellent border was drawn along the edges of the slide, and then the sections were rehydrated with PB. Endogenous peroxidases

were quenched with 0.05% hydrogen peroxide diluted in PB for 30 minutes. Sections were incubated with 5% goat serum in PB containing 0.1% Triton-X for 1 hour. Anti-Cntnap2 antibody was diluted to 1:1,000 in PB and applied to the sections overnight at 4°C . Sections were then incubated at room temperature with a biotinylated goat antirabbit secondary antibody (Table 2) at 1:200 in PB for 1 hour, washed, then incubated with avidin-biotin complex (VECTASTAIN Elite ABC Kit (Standard*), Vector Laboratories, Burlingame, CA) at 1:200 in PB with 0.1% Triton-X for 90 minutes. Sections were stained with fluorescein- or rhodamine-tyramide (Hopman et al., 1998) at 1:1,000 in PB with 0.1% Triton-X and 0.003% hydrogen peroxide. For double labeling, following Cntnap2 immunostaining, sections were incubated overnight at 4°C with either anti-NeuN or anti-parvalbumin antibodies (Table 1) at 1:1,000 in PB. Sections were then incubated at room temperature for 4 hours with antimouse Alexa Fluor 488, 555, or 568 (Table 2) diluted at 1:1,000 in PB. In the hippocampus, tyramide signal amplification was used for both labels. As above, peroxidase activity was quenched and sections were incubated with anti-NeuN at 1:500, then with antimouse HRP at 1:1,000 for 2 hours. These sections were then stained with rhodamine-tyramide as previously described. Peroxidases were quenched again with 0.3% hydrogen peroxide and Cntnap2 immunostaining followed as described above. Slides were mounted with glass coverslips using ProLong Gold antifade reagent (Life Technologies).

Surgical procedures

General methods

Adult male zebra finches were anesthetized with 2–4% isoflurane carried by oxygen using a Universal Vaporizer (Summit Anesthesia Support, Menlo Park, CA) for the duration of the surgery. The bird was placed on a homeothermic blanket mounted in a stereotaxic apparatus at a 45° head angle from the center of the ear bars to the tip of the beak. The cranial feathers were removed to expose the scalp, which was then cleansed using povidone-iodine. In order to preserve vascular

flow to the region, a semicircular incision was made originating and terminating at the caudal edge of the exposed scalp. The scalp was then folded back over a Gelitaspon (Gelita Medical, Amsterdam, Netherlands) moistened with sterile saline to expose the skull. Injections and recordings, described below, were made through $\sim 1 \text{ mm}^2$ windows cut in the skull. After each procedure the scalp was closed and sealed with Vet-bond (Fisher Scientific).

Retrograde targeting of RA projection neurons

An $\sim 1 \text{ mm}^2$ window was cut into the skull over the cerebellum $\sim 0.4 \text{ mm}$ from the midline, bilaterally. A carbon fiber electrode (Kation Scientific, Minneapolis, MN) was lowered into the brain 4.0 mm below the surface. Multiunit activity was amplified (A-M Systems, Sequim, WA), filtered (300 Hz highpass, 5 kHz lowpass), digitized at 20 kHz (Micro1401, CED, Cambridge, UK), and recorded with Spike 2 software (CED). The location of nXIIIs was determined by moving the electrode until multiunit activity corresponded to respiratory expiration. The carbon fiber electrode was then replaced with a glass electrode filled with Green Retrobeads IX (Lumafuor, Naples, FL). Retrobeads were injected into nXIIIs with a picospritzer (Toohey, Fairfield, NJ) 3 times on each side for 30 ms at 20 psi. Six days after the procedure each bird was euthanized and perfused with paraformaldehyde as described above.

LMAN lesions

A window was cut in the skull 5.15 mm rostral and 1.7 mm lateral of the midsagittal bifurcation for a unilateral injection. A glass electrode was filled with 10 mg/mL ibotenic acid (Fisher Scientific) in PB, pH 7.0, and lowered into the brain 2.0 mm from the surface to target LMAN and 96.6 nL were injected using a Nanoject II (Drummond Scientific, Broomall, PA). Four days after injection, birds were euthanized and brains collected and sectioned as described above. Sections containing LMAN were stained with thionin as described above to verify the extent of the lesion.

Cntnap2 protein quantification and analysis

Images were acquired using an Axio Imager.A1, with an AxioCam HRm digital camera or LSM 410 laser scanning confocal imager attached to an Axiovert 100 (Carl Zeiss, Oberkochen, Germany). Axiovision software (Carl Zeiss) was used to optimize photomicrographs to remove background, improve brightness and contrast, and to pseudocolor the images. For consistency, Cntnap2 is always represented here in green despite the true color of the fluorophore. In most cases, adjustments were made to the entire image and not to selec-

tive subregions, with the exception of the photomicrographs in Figure 2, in which artifacts of the immunostaining were removed. Anatomical regions were identified according to the published stereotaxic zebra finch brain atlas (<http://www.ncbi.nlm.nih.gov/books/NBK2348/>, courtesy of Dr. Barbara Nixdorf-Bergweiler and Hans-Joachim Bischof). ImageJ (Rasband, 1997–2012) was used to quantify Cntnap2-positive cells as follows. First, a border was drawn around RA based on the density of NeuN immunoreactivity. For areas outside of RA, a 600-pixel diameter circle was drawn laterally from RA in either the dorsal (AD) or ventral (AIV) part of the arcopallium. Within the border, all NeuN and Cntnap2-positive cells were counted. The total counts for each signal were adjusted using the Abercrombie method (Guillery, 2002) to reduce errors due to the 2D counting method. Each count was multiplied by the tissue thickness (T) and divided by the thickness plus the average diameter of the objects counted (T+d). This adjustment (T/(T+d)) was calculated separately for each section analyzed, and reduced the raw counts by 11–33%, with an average of 24%. To control for the different sizes of RA across sections and animals, statistical significance was determined by nonparametric resampling (bootstrapping) of the ratios of Cntnap2 to NeuN counts. This was done in two stages. First, a modified two-way analysis of variance (ANOVA) compared sex, age, and the interaction effect. A Fisher's F statistic was calculated for each of the groups, then the groups were pooled and data were sampled with replacement 10,000 times, generating a range of pseudo-F statistics. Statistical significance was achieved when the F statistic from the real data was greater than 95% ($P < 0.05$) or 99% ($P < 0.01$) of the pseudo-statistics. Then, for groups with an ANOVA P -value below 0.05, modified Student's t -tests were performed for individual groups with the same resampling protocol as described for ANOVA, instead using a Student's t statistic.

RESULTS

Antibody validation

Bioinformatic analysis revealed that the C-terminus of Cntnap2 is highly conserved between humans and zebra finches (Panaitof et al., 2010), and that the last 76 amino acids are identical (amino acids 1255–1331 in human, 1252–1328 in zebra finch: GVNRSALIGGVIAVVIFTILCTLVFLIRYMFRRHKGTYHTNEAKGAESAESADAAIMNNDPNFTETIDESKKEWLI). A commercial antibody available from Millipore and raised against C-terminus amino acids 1315–1331 of human CNTNAP2 (1312–1328 of zebra finch Cntnap2) was thus selected to test its

ability to specifically detect the zebra finch isoform. In western analyses of zebra finch whole brain homogenate, this antibody detects a single prominent band at the predicted molecular weight of ~180 kDa. PreadSORption of the antibody with the antigenic peptide considerably decreases the intensity of this band (Fig. 2A). The specificity of the antibody was further validated by overexpressing zebra finch *Cntnap2* (accession number NM_001193337.1) in ZFTMA cells (Itoh and Arnold, 2011), a zebra finch immortalized cell line that does not endogenously express the protein. Cultures transfected with zebra finch *Cntnap2* produce the same protein band, whereas those from untransfected cultures (not shown) or transfected with a control construct containing sequences coding only for GFP do not (Fig. 2B). Specificity of the antibody was again confirmed by preadsorption (see Materials and Methods).

The Millipore antibody was subsequently tested for use in immunohistochemistry. In mammals, *Cntnap2* is expressed in axons of myelinated nerves, colocalized with VGKC subunits (Poliak et al., 1999, 2001, 2003; Gu and Gu, 2011). To verify that the Millipore antibody detects zebra finch *Cntnap2* in situ, we immunostained optic (Fig. 2C–E) and sciatic (Fig. 2D–F) nerves dissected from zebra finches for both *Cntnap2* and Kv β 2. In both nerve preparations, the signals from the two antibodies overlap, as evidenced by the colocalization tools in ImageJ, further confirming that the antibody specifically detects zebra finch *Cntnap2*.

Cntnap2 protein distribution in the zebra finch brain

Similar to reported mammalian data (Poliak et al., 1999), *Cntnap2* distribution is extensive in zebra finch brains, although not expressed to the same level in all regions. Particular enrichment is observed in myelinated areas consistent with axonal expression, such as the fronto-arcopallial tract, optic tract, optic chiasm (not shown), the lateral forebrain bundle (Fig. 3A–C), and layer 5 of the optic tectum (Fig. 3D–F). In the cerebellum, the Purkinje cell layer is marked by intense *Cntnap2* immunostaining of cell bodies, and fibers containing *Cntnap2* can be observed in the cerebellar white matter. Much less *Cntnap2* is found in the granular and molecular layers (Fig. 3G–I). In the midbrain, *Cntnap2* is found in the parvocellular portion of the isthmus nucleus (not shown). Thalamic regions containing high levels of *Cntnap2* include the anterior dorsomedial nucleus, dorsal portion of the lateral mesencephalic nucleus, rotund nucleus, lateral spiriform nucleus, and pretectal nucleus. In the telencephalon, enrichment of *Cntnap2* is found in the entopallium, the anterior hyper-

pallium, striatopallidum, globus pallidus, field L (not shown), and cell bodies resembling pyramidal neurons (Montagnese et al., 1996) in the medial hippocampus (Fig. 3J–L).

Within the song circuit of an adult male zebra finch, *Cntnap2* protein distribution generally follows the mRNA distribution reported in Panaitof et al. (2010), with some exceptions. Although cortical nucleus HVC does contain *Cntnap2*-positive cells, expression is not enriched relative to the surrounding nidopallium (Fig. 4A–C). As with the mRNA, cortical nuclei RA (Fig. 4D–F) and LMAN (Fig. 4G–I) have elevated *Cntnap2* levels relative to the surrounding arco- and nidopallium, respectively. In contrast with the reported mRNA levels, the basal ganglia song control region, area X, exhibits greater *Cntnap2* protein expression than the surrounding striatopallidum (Fig. 4J–L). The *Cntnap2* protein in the aforementioned areas is present not only on cell bodies, but also in the neuropil. The thalamic song nucleus DLM, however, has *Cntnap2*-positive cell bodies, but relatively less protein in the neuropil than the surrounding thalamic regions (Fig. 4M–O).

Sexually dimorphic expression of Cntnap2 in RA

Cntnap2 mRNA expression is sexually dimorphic in LMAN and RA in developing zebra finches. Males have slightly more *Cntnap2* in LMAN than females throughout development, although the level of expression increases in both sexes with age. There is a more striking difference in expression in RA at 50d. Similar *Cntnap2* levels are detected in both sexes prior to 35d. Between the two timepoints, expression in females begins to decrease, while males maintain a high level through adulthood (Panaitof et al., 2010). We therefore compared levels of *Cntnap2* immunostaining in RA in both sexes at developmental timepoints within sensory acquisition and sensorimotor learning periods, and after song crystallization (males, Fig. 5A–E; females, Fig. 5F–J). At 25 and 35d leading up to the onset of sensorimotor learning, the fraction of RA neurons that are positive for *Cntnap2* are comparably enriched in both sexes relative to the surrounding dorsal and ventral intermediate arcopallium (AD and AIV, respectively). However, by 50d the fraction of *Cntnap2*-positive neurons in female RA significantly decreases (Fig. 5L), and falls to levels comparable to those in AD and AIV (Fig. 5M,N). This timepoint falls within the sensorimotor phase of vocal learning, during which males practice their memorized song (Eales, 1985). Male *Cntnap2* enrichment in RA is maintained throughout development and into adulthood and crystallization of song, whereas in females it is

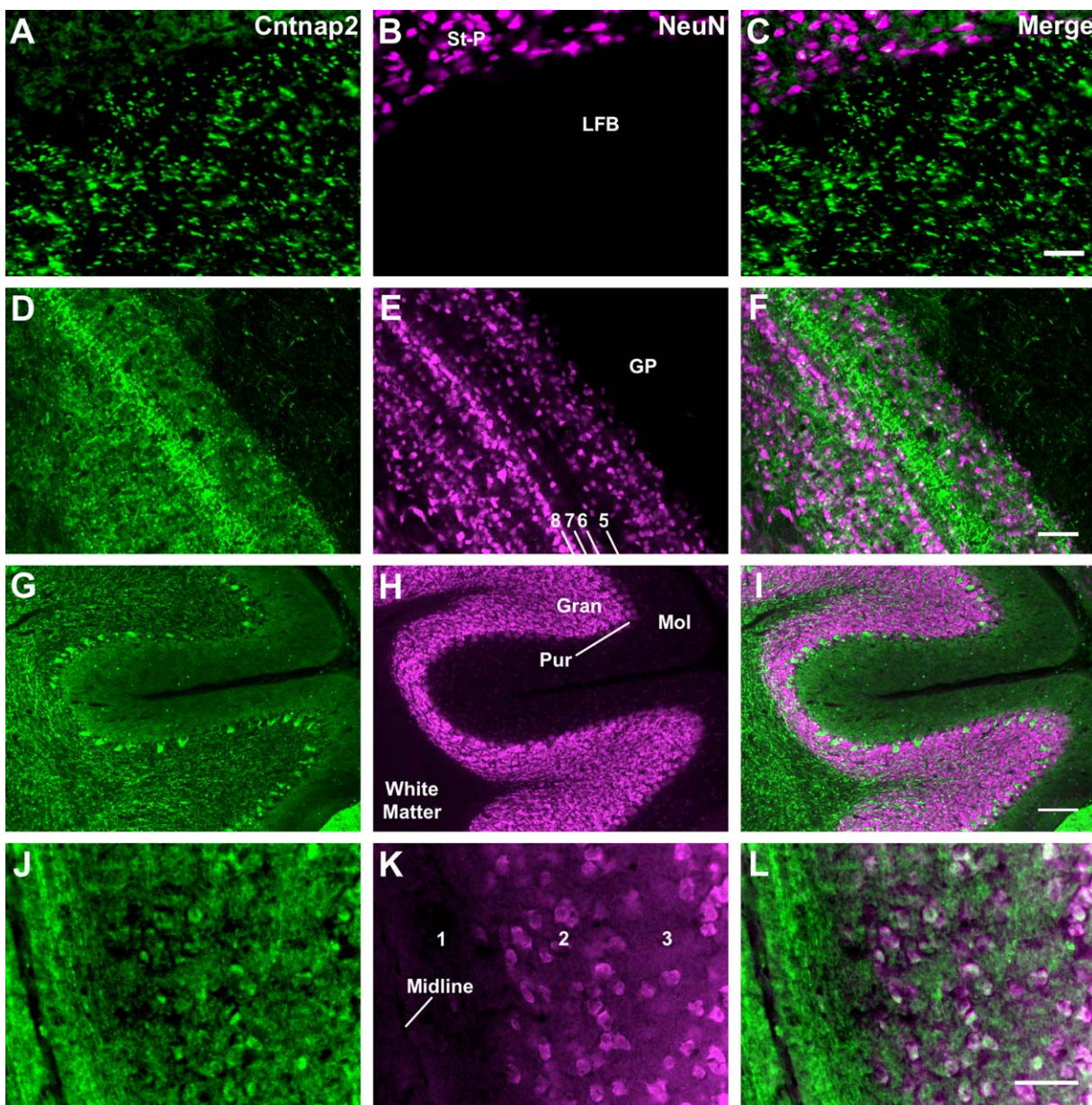


Figure 3. Cntnap2 distribution in nonsong circuit brain regions. Cntnap2 is detected in several areas outside the song circuit of the zebra finch brain, including in structures reported to express Cntnap2 in rodents (Poliak et al., 1999). Nonsong circuit tissue in this figure are taken from regions depicted in Figure 1B. Neuron-specific marker NeuN (magenta) is used for reference. **A–C:** Axonal patterning of Cntnap2 label in the lateral forebrain bundle within the telencephalon. **D–F:** intense Cntnap2 (green) labeling along axons in layer 5 of the optic tectum. Numbers in (B) indicate the layers of the optic tectum according to Ramón y Cajal (1911). **G–I:** Purkinje cell bodies and the cerebellar white matter strongly express Cntnap2, with less in the molecular layer, and fibrous signal in the granular layer and white matter. **J–L:** Coronal section of the medial hippocampus; numbers indicate layers (Montagnese et al., 1996). Cntnap2 marks neuronal somata in the pyramidal cell region (white arrows). See list for abbreviations. Scale bars = 50 μ m in A–C; 200 μ m in D–L. [Color figure can be viewed in the online issue, which is available at wileyonlinelibrary.com.]

significantly reduced. The difference in Cntnap2 protein expression within the arcopallium between males and females and at different developmental stages appears unique to RA. A comparison of the number of Cntnap2-enriched cells in AD and AIV reveals no significant effect of age or sex (Fig. 5M,N).

LMAN projections contribute to Cntnap2 expression in RA

To test the possible contribution of LMAN terminals to Cntnap2 in RA, LMAN was unilaterally lesioned using ibotenic acid in three adult males (Fig. 6A–C, D–F, G–I). The resulting Cntnap2 protein expression was observed

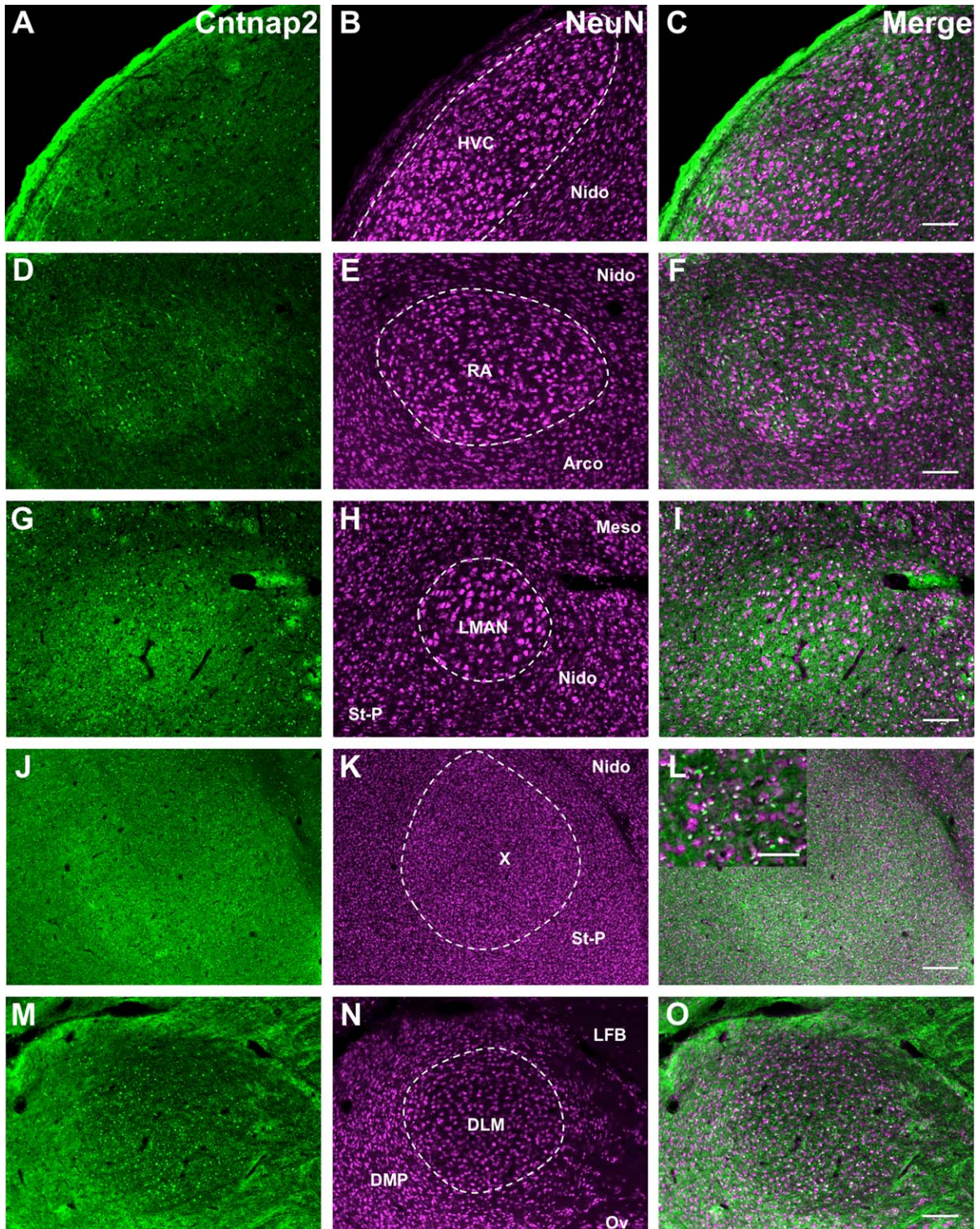


Figure 4. Cntnap2 protein in song circuit nuclei. Fluorescent photomicrographic images of song control nuclei. Cntnap2 signals are in green, and NeuN signals in magenta. **A–C:** HVC in the nidopallium; **D–F:** RA in the arcopallium; **G–I:** LMAN in the nidopallium; **J–L:** Area X in the striatopallidum, inset: higher magnification inside X. **M–O:** DLM in the thalamus, along with the ovoid nucleus, the dorsomedial nucleus of the posterior thalamus, and the lateral forebrain bundle. Each nucleus is indicated by dashed line traces on the NeuN (middle column) panels. Greater Cntnap2 labeling is found within RA, LMAN, and area X relative to surrounding brain regions on both cell bodies and in the neuropil. HVC and DLM contain Cntnap2-expressing cells, but with expression levels comparable to their surrounding tissues. See list for abbreviations. Scale bars = 200 μ m A–I; in 100 μ m in J–L (50 μ m inset); 200 μ m in M–O. [Color figure can be viewed in the online issue, which is available at wileyonlinelibrary.com.]

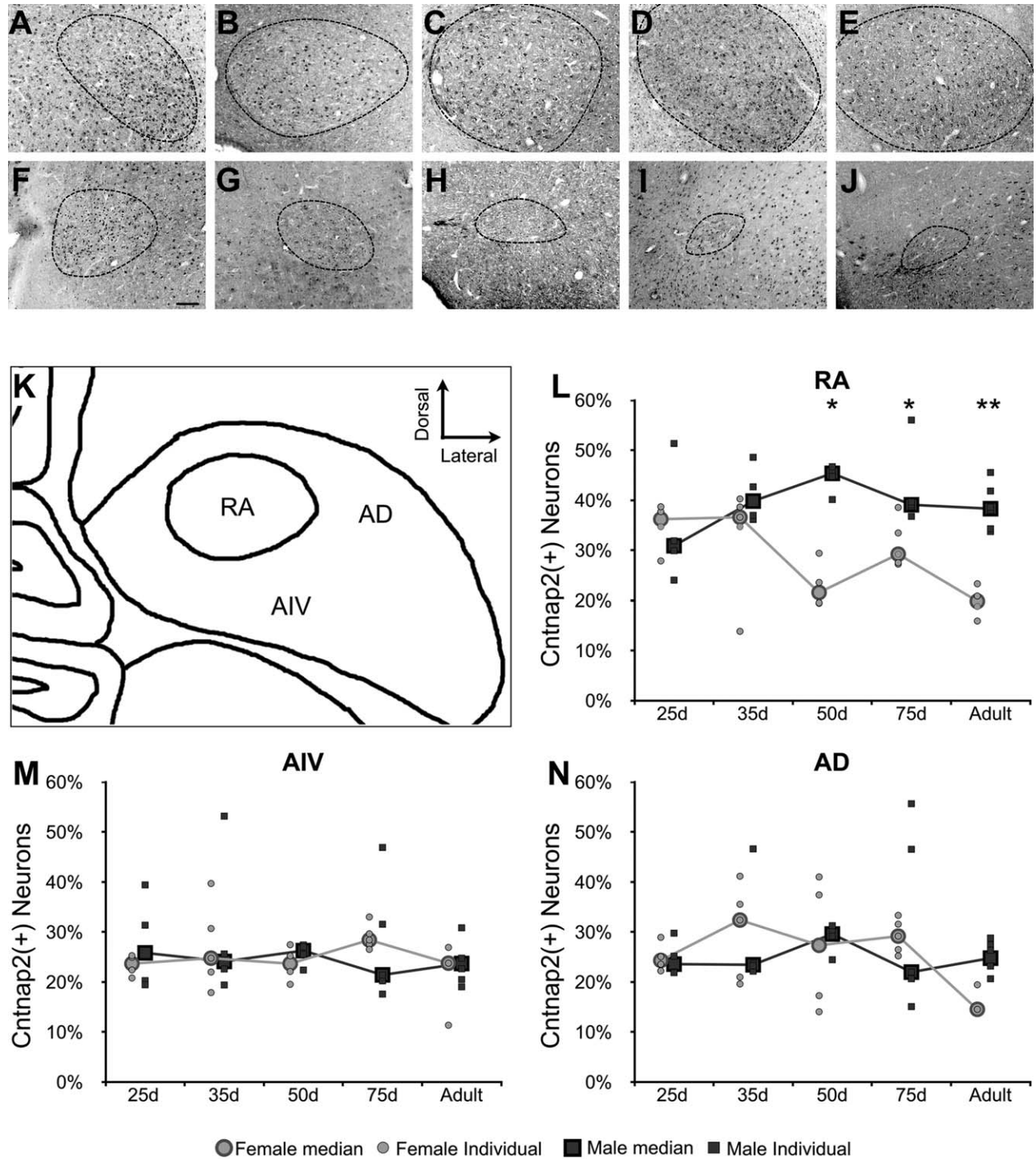


Figure 5. Cntnap2 within RA in both sexes at developmental timepoints during male song learning. **A–J:** Representative images of Cntnap2 immunolabeling of cells in male (A–E) and female (F–J) RA at timepoints during development encompassing the onset of sensory acquisition, sensorimotor learning, and crystallization of song. Anti-NeuN signals (not shown) were used to trace the border of RA in each image. As previously reported (Konishi and Akutagawa, 1985; Nixdorf-Bergweiler, 1996), the size of RA begins to decrease in females and increase in males starting around 35d and continues through development until maturity. **K:** A diagram of RA and the two arcopallial regions in which labeled cells were counted: the ventral intermediate arcopallium (AIV) and the dorsal arcopallium (AD). **L–N:** Graphs representing the percentage of Cntnap2-positive neurons out of the total number of NeuN-positive cells found in RA, AIV, and AD, respectively, for 3–6 birds of each sex at each timepoint. Statistical significance was determined by resampling ANOVA, followed by individual Student's *t*-tests **P* < 0.05, ***P* < 0.01. See list for abbreviations. Scale bar = 100 μ m.

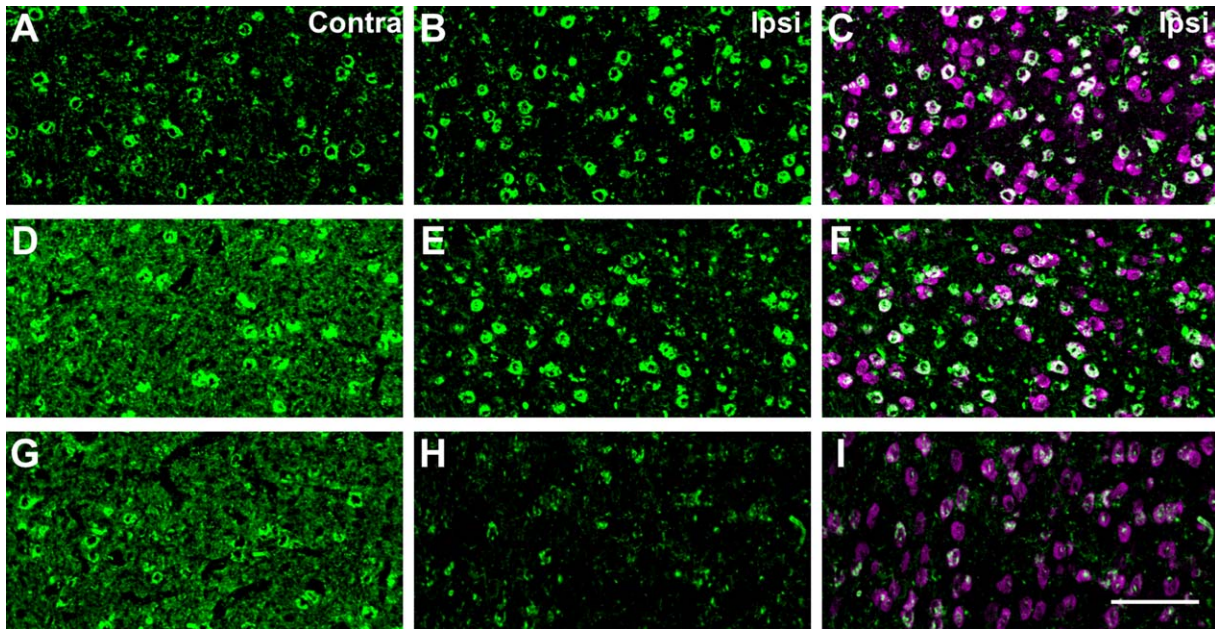


Figure 6. Unilateral LMAN lesions result in an ipsilateral decrease of Cntnap2 in RA. Representative photomicrographic images of Cntnap2 labeling (green) in RA from three adult male zebra finches (A–C, D–F, G–I) in which LMAN was lesioned unilaterally by injection of ibotenic acid. Double labeling with NeuN (magenta; C,F,I) indicates neuronal cell bodies. In all cases, the lesion reduces the amount of Cntnap2 in the neuropil, but not cell bodies, in ipsilateral RA relative to the contralateral nucleus, indicating that some of the Cntnap2 in the neuropil originates from LMAN projections. See list for abbreviations. Scale bar = 25 μm . [Color figure can be viewed in the online issue, which is available at wileyonlinelibrary.com.]

in the ipsilateral RA and compared to that in the non-lesioned contralateral side. Somatic expression of Cntnap2 remained unaffected in the ipsilateral RA, but there was a decrement in immunostaining intensity in the neuropil compared with the contralateral RA, suggesting that some of the Cntnap2 is indeed from LMAN projections. In summary, within the vocal production circuit, Cntnap2 enrichment appears to be most prominent in RA and due to expression in both neuronal somata and neuropil, including that arising from within LMAN nerve terminals.

Cntnap2 is expressed in RA projection neurons

Within RA, Cntnap2 somal expression is restricted to a subset of the neuronal phenotypes. At least two distinct neuronal populations in RA have been defined based on their electrophysiological signatures and morphology: GABAergic interneurons, and glutamatergic projection neurons (Spiro et al., 1999). The latter directly synapse onto neurons within nXllts, which directly innervates the syrinx. Parvalbumin staining has been used to differentiate these two types. Whereas some interneurons stain intensely for parvalbumin, projection neurons stain relatively weakly (Wild et al., 2001). To determine whether Cntnap2 is expressed in projection neurons, flu-

orescent retrobeads were injected into nXllts (Fig. 7A–C). Following retrograde transport, fluorescent signals colocalized with Cntnap2 signals in RA (Fig. 7D–F), but not in cells that expressed a high level of parvalbumin (Fig. 7G–I). Rather, we found that Cntnap2 signals overlapped only with weakly parvalbumin-positive neurons, consistent with the interpretation that RA projection neurons express Cntnap2 (Fig. 7J–L). The overlap of retrobeads with Cntnap2 signals further supports the hypothesis that Cntnap2 is expressed in RA neurons which project to nXllts.

DISCUSSION

Here we have characterized the protein distribution of Cntnap2, a molecule linked to human language disorders, in the brain of a nonhuman vocal learner, the zebra finch species of songbird. Because the neurons that are dedicated to vocal learning are clustered together in the songbird brain (Fig. 1), this analysis enables direct comparison of Cntnap2 levels within song-dedicated neurons relative to their levels in surrounding tissues, which, although made up of similar cell types, contribute to nonvocal-related functions. Moreover, the sexual dimorphism of vocal learning and the underlying song control circuitry allow us to compare protein expression between vocal and nonvocal learners within the same species.

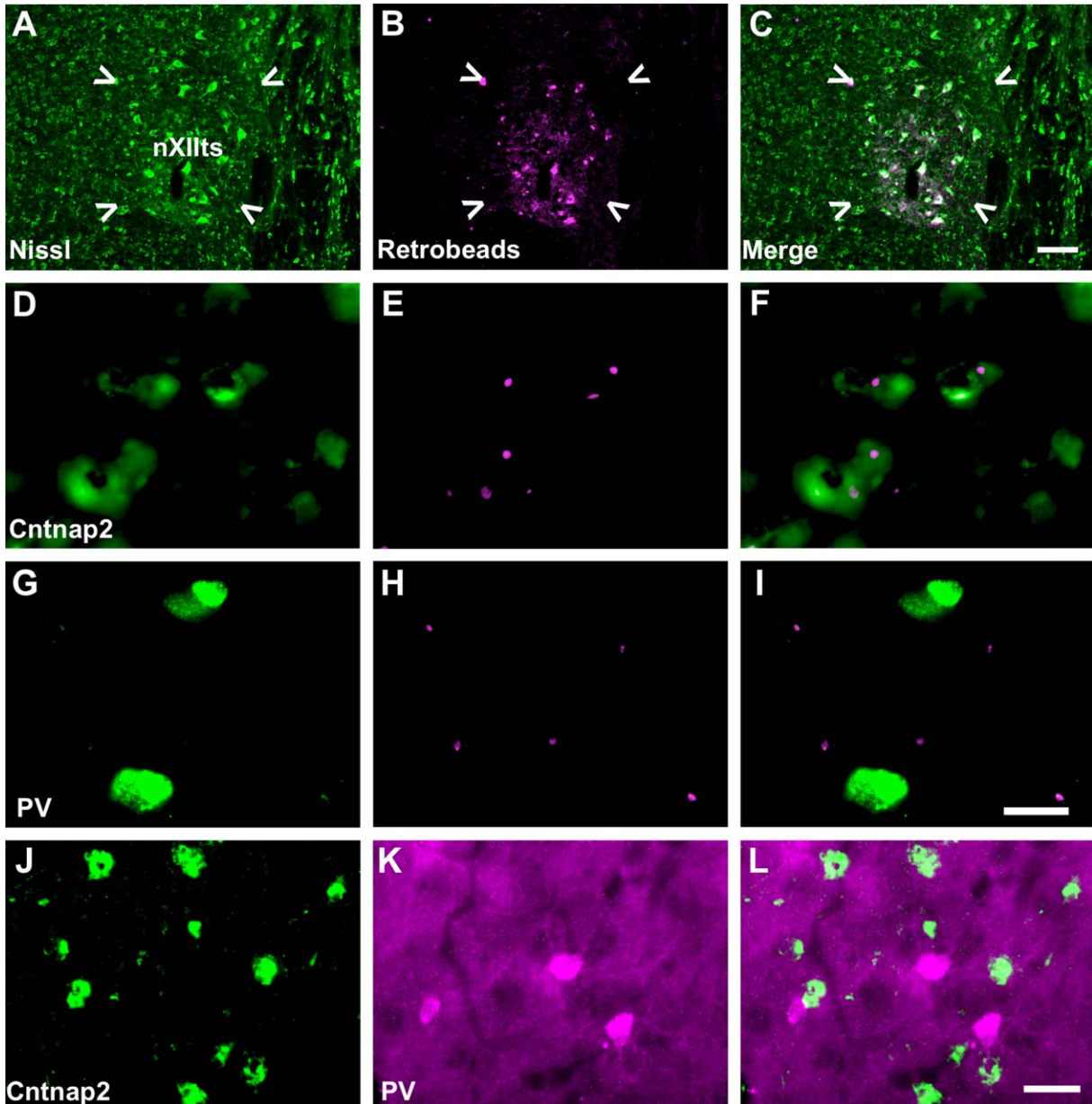


Figure 7. Cntnap2 is expressed in RA projection neurons, not parvalbumin-positive interneurons. **A–C:** Injection site of retrobeads (magenta) in nXIIIs (indicated by white arrows), identified by Nissl stain (green). **D–F:** Retrobeads overlap with Cntnap2 (green) expressing cells in RA. **G–I:** Retrobeads do not overlap with strongly parvalbumin positive interneurons. **J–L:** Cntnap2 immunolabeling (green) does not overlap with RA inhibitory interneurons intensely labeled with parvalbumin (magenta). Retrograde labeling reveals that RA projection neurons express Cntnap2 and confirms its absence in parvalbumin-positive interneurons. See list for abbreviations. Scale bars = 50 μ m in A–C; 20 μ m in D–I; 25 μ m in J–L. [Color figure can be viewed in the online issue, which is available at wileyonlinelibrary.com.]

We can further draw parallels between humans and songbirds by investigating the cell types within a song nucleus in which we detect Cntnap2 expression.

Outside the song circuit, immunoreactivity is widespread throughout the telencephalon with areas of particularly high expression, such as in myelinated regions, and in the Purkinje cell layer of the cerebellum, and in pyramidal-like cells (Montagnese et al., 1996) in layers 2 and 3 of the hippocampus (Fig. 3), similar to that

described for mammals (Poliak et al., 1999). Notably, however, expression within several nuclei of the song circuit in the adult brain is strikingly different than in their respective surrounding regions, which are not part of the song control circuitry (Fig. 4). In the AFP, Cntnap2 protein is enriched in cortical LMAN relative to the anterior nidopallium, in area X relative to the striatopallidum, and in the somata of DLM relative to the anterior thalamus. Although enrichment in LMAN and

DLM is expected based on the mRNA data, the enrichment in area X is surprising given the lower transcript levels in this region relative to the surrounding striatopallidum (Panaitof et al., 2010). *Cntnap2* protein is found in the neuropil of area X, leaving open the possibility that some of the protein arises from HVC and/or LMAN terminals, similar to the contribution of LMAN to *Cntnap2* expression in RA (Fig. 6). There is also somal *Cntnap2* expression, suggesting at least some protein originates in area X. The difference between the observed mRNA and protein data may reflect state-dependent regulation of the protein, perhaps by transcription factors such as FoxP2 (Teramitsu and White, 2006; Miller et al., 2008). Whether *Cntnap2* is a direct target of FoxP2 in zebra finches, as it is in humans (Vernes et al., 2008), remains to be tested. The zebra finch genomic *Cntnap2* sequence (RefSeq assembly ID GCF_000151805.1) contains many potential FoxP2 binding sites (Stroud et al., 2006), mostly in the first intron. The FOXP2 binding site in humans was confirmed to be in the first intron by chromatin immunoprecipitation (Vernes et al., 2008). The lower mRNA levels and higher protein in area X thus likely reflect a combination of cellular trafficking, transcriptional and posttranscriptional regulation. Whatever the mechanism, *Cntnap2* mRNA and protein expression within the nucleus differs from levels in the surrounding tissue, despite the similar cell type composition of these subregions.

Cntnap2 protein distribution in the posterior pathway is similar to that for the mRNA. The amount within HVC is comparable to the surrounding nidopallium, whereas it is enriched in RA of males and juvenile females (Panaitof et al., 2010). The connectivity of the posterior vocal pathway in males suggests that RA-projecting neurons in HVC are analogous to mammalian neurons in cortical layer 2/3, which do not show prominent *Cntnap2* staining, whereas RA projection neurons are analogous to mammalian cortical layer 5 pyramidal neurons (Jarvis, 2004), which exhibit prominent *Cntnap2* levels (Poliak et al., 1999). The projection from RA to nXllts is a corticospinal connection shared with mammalian motor cortex and is hypothesized to allow direct activation of individual muscles necessary for fine motor control (Vicario, 1991). Notably, these direct connections onto motor neurons controlling the muscles involved in phonation are posited to enable the vocal learning capacity of select species such as humans and songbirds (Jürgens, 2009; Arriaga et al., 2012). Overlap of retrobeads injected into nXllts in RA and *Cntnap2*-positive neurons (Fig. 7) indicates that *Cntnap2* is present in this connection, raising the possibility that *Cntnap2* is required for its establishment and/or proper function. Additionally, the reduction of *Cntnap2* in the neuropil of RA following an ipsilateral LMAN lesion (Fig. 6) suggests

that some of the enrichment in RA is provided from LMAN projections. This long-range connection is reminiscent of the connectivity that is altered in humans bearing the *CNTNAP2* risk alleles for ASD and SLI who exhibit increased local and decreased long-range connectivity of the medial prefrontal cortex (mPFC), and less lateralization than their nonrisk allele counterparts (Scott-Van Zeeland et al., 2010). In fact, LMAN is postulated to be homologous to human PFC based on shared physiologic and anatomic features including connectivity (Kojima et al., 2013). Taken together, these parallel observations in humans and songbirds support the idea that *Cntnap2* affects neural connectivity critical for vocal learning across taxonomic classes.

This hypothesis is further supported by the sexually dimorphic expression in zebra finch brain. Similar to that reported for *Cntnap2* mRNA, males and females share protein enrichment in RA early in development. However, by 50d the enrichment in female RA wanes, whereas it persists in males throughout adulthood. Since *Cntnap2* is similarly enriched in RA in males and females prior to 50 days, the sexual dimorphism may reflect a change in cell composition in RA or a sex-based difference in gene expression within each cell. These data demonstrate a loss of *Cntnap2*-labeled cells in female RA with age. This may be due to preferential apoptosis (Konishi and Akutagawa, 1990) of neurons that express *Cntnap2* or downregulation of both *Cntnap2* mRNA and protein in female zebra finches, who do not use this nucleus for producing learned vocalizations. In mammals, some sex-typical behaviors have been associated with sexually dimorphic expression of individual genes, supporting the hypothesis that sex-related behaviors driven by hormones are mediated in part by genes (Xu et al., 2012) or in fact by genes independent of hormones (Arnold et al., 2013). In the case of the zebra finch, genes that exhibit sexually dimorphic expression in song circuitry are likely to be involved, perhaps even crucial, for singing. These same genes may also be involved in human speech and language. This hypothesis was the basis for the prediction that FOXP1 mutations would impair human speech. FOXP1 is a transcription factor closely related to FOXP2, and the two form heterodimers to control gene expression. Sexually dimorphic expression of *FoxP1*, but not *FoxP2*, was found in the song circuit of quiescent zebra finches, leading to the aforementioned prediction (Teramitsu et al., 2004). Subsequently, several cases were described of FOXP1 mutations in people with language disorders (Pariani et al., 2009; Carr et al., 2010; Hamdan et al., 2010; Palumbo et al., 2012). The sexually dimorphic expression of *Cntnap2* in RA also fits this pattern, and may in fact be regulated by FoxP1 in tandem or independent from FoxP2.

What might be the mechanistic function of Cntnap2 in the song circuit, or RA specifically? Cntnap2 is closely related to the neurexins, which have also been implicated in ASD (Südhof, 2008). Although neurexins function at the synapse, Cntnap2 is found at the juxtaparanodes of myelinated axons. There, it is responsible for the clustering of *Shaker*-type VGKCs (Poliak et al., 1999, 2003; Horresh et al., 2008). Selective blockade of these channels on axons from rat central nervous system during myelination early in development leads to aberrant action potential waveforms. However, when the animal becomes mature application of the blocker no longer affects the waveform (Devaux et al., 2002). In songbirds, all song circuit nuclei send and receive long-range connections, which may require Cntnap2 at a macrocircuit level to cluster VGKCs at juxtaparanodes in order to establish and/or maintain synaptic connections required for learning and producing vocalizations. Loss of Cntnap2 in the neuropil of RA following LMAN lesion is evidence for a macrocircuit role for Cntnap2 in this cortical–cortical connection. This suggests that if the role of Cntnap2 in clustering VGKCs is important for vocal learning, it will have the greatest impact early in development, while the process of myelination is still ongoing. Cntnap2 may have additional, yet unknown functions, suggested by *CNTNAP2* enrichment in human embryonic cortex well before myelination (Abrahams et al., 2007). Recent evidence suggests that Cntnap2 may influence synaptic connectivity, increasing cell-autonomous dendritic arborization and the number of synaptic sites in cultured neurons. Contactin 2, the binding partner of Cntnap2, appears to have the opposite effect on synaptic connectivity (Anderson et al., 2012). Contactin 2 and Cntnap2 together may affect the development of brain areas related to vocal learning and language. Cntnap2 may be important for microcircuit connectivity in song nuclei of the adult zebra finch brain as well, by establishing and maintaining local connections within each nucleus through increasing dendritic arborization and the number of active postsynaptic connections. According to this hypothesis, we expect that loss of Cntnap2 in male RA before the onset of sensorimotor learning would lead to fewer connections with HVC and an impaired ability to mimic the tutor's song.

Further investigation into the role of Cntnap2 in vocal learning in songbirds will certainly benefit our understanding of human speech disorders associated with risk variants of the gene, as well as the neurobiology of language as a whole. Taking advantage of the well-characterized song circuitry, an individual song nucleus could be targeted for Cntnap2 RNA interference. If Cntnap2 is involved in song learning, as it seems to be in human speech, we expect knock-

down to impair vocal learning in juvenile males, whose songs have not yet crystallized. This system may also be used to parse the activational versus organizational effects of Cntnap2 in vocal learning by manipulating Cntnap2 levels at different times during development. Besides behavior, we additionally expect to find neurophysiological changes. Knocking down Cntnap2 in RA may result in a mislocalization of potassium channels, which could slow the repolarization phase of an action potential similar to the effects of blocking those channels, particularly prior to the completion of myelination (Devaux et al., 2002). There may also be changes to synaptic connectivity between RA and HVC or LMAN concurrent with decreased dendritic arborization of projection neurons originating in RA, similar to the effects reported in vitro reported by Anderson et al. (2012). Reducing Cntnap2 levels in LMAN may augment its local connectivity and decrease its long-range connectivity to RA, similar to the altered connectivity in forebrains of humans with risk variants of Cntnap2 (Scott-Van Zeeland et al., 2010). The balance between inhibition and excitation is also likely to be affected, as it is in cases of autism (Cline, 2005) and *Cntnap2* knockout mouse models (Peñagarikano et al., 2011). The present and future investigation into the role of Cntnap2 in vocal learning using songbirds complements studies in mammals moving toward a better understanding of its associated disorders in humans.

ACKNOWLEDGMENTS

The authors thank Melissa Coleman and Felix Schweizer for assistance in the use of their equipment for retrograde labeling and confocal fluorescence imaging, respectively. Brett Abrahams and Hongmei Dong provided the zebra finch Cntnap2 cDNA construct used in tests of antibody specificity. Yuichiro Itoh and Arthur Arnold provided the ZFTMA cell line. Vijayendran Chandran identified potential FoxP2 binding sites in zebra finch Cntnap2. We thank Alice Fleming for advice on immunohistochemistry and Julie Miller for revising drafts of the article and guidance on the methodology used within. We also thank Dorsa Beroukhim, Guillermo Milian, and Diana Sanchez for assistance with collecting tissue samples. The authors thank two anonymous reviewers for constructive comments.

CONFLICT OF INTEREST

The authors declare they have no conflict of interest.

ROLE OF AUTHORS

Both authors had full access to all the data in the study and take responsibility for the integrity of the data and the accuracy of the data analysis. Study

concept and design: MCC and SAW. Acquisition of data: MCC. Analysis and interpretation of data: MCC. Drafting the article: MCC. Critical revision of the article for important intellectual content: SAW. Statistical analysis: MCC. Obtained funding: MCC and SAW. Administrative, technical, and material support: SAW. Study supervision: SAW.

LITERATURE CITED

- Abrahams BS, Tentler D, Perederiy JV, Oldham MC, Coppola G, Geschwind DH. 2007. Genome-wide analyses of human perisylvian cerebral cortical patterning. *Proc Natl Acad Sci U S A* 104:17849–17854.
- Alarcón M, Abrahams BS, Stone JL, Duvall JA, Perederiy JV, Bomar JM, Sebat J, Wigler M, Martin CL, Ledbetter DH, et al. 2008. Linkage, association, and gene-expression analyses identify CNTNAP2 as an autism-susceptibility gene. *Am J Hum Genet* 82:150–159.
- Anderson GR, Galfin T, Xu W, Aoto J, Malenka RC, Südhof TC. 2012. Candidate autism gene screen identifies critical role for cell-adhesion molecule CASPR2 in dendritic arborization and spine development. *Proc Natl Acad Sci U S A* 109:18120–18125.
- Arking DE, Cutler DJ, Brune CW, Teslovich TM, West K, Ikeda M, Rea A, Guy M, Lin S, Cook EH, Chakravarti A. 2008. A common genetic variant in the neurexin superfamily member CNTNAP2 increases familial risk of autism. *Am J Hum Genet* 82:160–164.
- Arnold AP, Chen X, Link JC, Itoh Y, Reue K. 2013. Cell-autonomous sex determination outside of the gonad. *Dev Dyn* 242:371–379.
- Arriaga G, Zhou EP, Jarvis ED. 2012. Of mice, birds, and men: the mouse ultrasonic song system has some features similar to humans and song-learning birds. *PLoS ONE* 7:e46610.
- Brainard MS, Doupe AJ. 2000. Auditory feedback in learning and maintenance of vocal behaviour. *Nat Rev Neurosci* 1:31–40.
- Carr CW, Moreno-De-Luca D, Parker C, Zimmerman HH, Ledbetter N, Martin CL, Dobyns WB, Abdul-Rahman OA. 2010. Chiari I malformation, delayed gross motor skills, severe speech delay, and epileptiform discharges in a child with FOXP1 haploinsufficiency. *Eur J Hum Genet* 18:1216–1220.
- Celio MR, Baier W, Schärer L, de Viragh PA, Gerday C. 1988. Monoclonal antibodies directed against the calcium binding protein parvalbumin. *Cell Calcium* 9:81–86.
- Cline H. 2005. Synaptogenesis: a balancing act between excitation and inhibition. *Curr Biol* 15:R203–5.
- Devaux J, Gola M, Jacquet G, Crest M. 2002. Effects of K⁺ channel blockers on developing rat myelinated CNS axons: identification of four types of K⁺ channels. *J Neurophysiol* 87:1376–1385.
- Eales LA. 1985. Song learning in zebra finches: some effects of song model availability on what is learnt and when. *Anim Behav* 33:1293–1300.
- Fitch WT. 2012. Evolutionary developmental biology and human language evolution: constraints on adaptation. *Evol Biol* 39:613–637.
- Fortune T, Lurie DI. 2009. Chronic low-level lead exposure affects the monoaminergic system in the mouse superior olivary complex. *J Comp Neurol* 513:542–558.
- Graham SA, Fisher SE. 2013. Decoding the genetics of speech and language. *Curr Opin Neurobiol* 23:43–51.
- Gu C, Gu Y. 2011. Clustering and activity tuning of Kv1 channels in myelinated Hippocampal axons. *J Biol Chem* 286:25835–25847.
- Guillery RW. 2002. On counting and counting errors. *J Comp Neurol* 447:1–7.
- Hamdan FF, Daoud H, Rochefort D, Piton A, Gauthier J, Langlois M, Foomani G, Dobrzyniecka S, Krebs M-O, Joober R, Lafrenière RG, Lacaille JC, Mottron L, Drapeau P, Beauchamp MH, Phillips MS, Fombonne E, Rouleau GA, Michaud JL. 2010. De novo mutations in FOXP1 in cases with intellectual disability, autism, and language impairment. *Am J Hum Genet* 87:671–678.
- Hilliard AT, Miller JE, Fraley ER, Horvath S, White SA. 2012. Molecular microcircuitry underlies functional specification in a basal ganglia circuit dedicated to vocal learning. *Neuron* 73:537–552.
- Hopman AHN, Ramaekers FCS, Speel EJM. 1998. Rapid synthesis of biotin-, digoxigenin-, trinitrophenyl-, and fluorochrome-labeled tyramides and their application for in situ hybridization using CARD amplification. *J Histochem Cytochem* 46:771–777.
- Horresh I, Poliak S, Grant S, Bredt D, Rasband MN, Peles E. 2008. Multiple molecular interactions determine the clustering of Caspr2 and Kv1 channels in myelinated axons. *J Neurosci* 28:14213–14222.
- Immelmann K. 1969. Song development in the zebra finch and other estrildid finches. In: Hinde RA, editor. *Bird vocalizations*. Cambridge, UK: Cambridge University Press. p 61–74.
- Itoh Y, Arnold AP. 2011. Zebra finch cell lines from naturally occurring tumors. *In Vitro Cell Dev Biol Anim* 47:280–282.
- Jarvis ED. 2004. Learned birdsong and the neurobiology of human language. *Ann N Y Acad Sci* 1016:749–777.
- Jones LG, Prins J, Park S, Walton JP, Luebke AE, Lurie DI. 2008. Lead exposure during development results in increased neurofilament phosphorylation, neuritic beading, and temporal processing deficits within the murine auditory brainstem. *J Comp Neurol* 506:1003–1017.
- Jürgens U. 2009. The neural control of vocalization in mammals: a review. *J Voice* 23:1–10.
- Knornschild M, Nagy M, Metz M, Mayer F, Helversen von O. 2010. Complex vocal imitation during ontogeny in a bat. *Biol Lett* 6:156–159.
- Kojima S, Kao MH, Doupe AJ. 2013. Task-related “cortical” bursting depends critically on basal ganglia input and is linked to vocal plasticity. *Proc Natl Acad Sci U S A* 110:4756–4761.
- Konishi M, Akutagawa E. 1985. Neuronal growth, atrophy and death in a sexually dimorphic song nucleus in the zebra finch brain. *Nature* 315:145–147.
- Konishi M, Akutagawa E. 1990. Growth and atrophy of neurons labeled at their birth in a song nucleus of the zebra finch. *Proc Natl Acad Sci U S A* 87:3538–3541.
- Lai CS, Fisher SE, Hurst JA, Vargha-Khadem F, Monaco AP. 2001. A forkhead-domain gene is mutated in a severe speech and language disorder. *Nature* 413:519–523.
- Li X, Hu Z, He Y, Xiong Z, Long Z, Peng Y, Bu F, Ling J, Xun G, Mo X, Mo X, Pan Q, Zhao J, Xia K. 2010. Association analysis of CNTNAP2 polymorphisms with autism in the Chinese Han population. *Psychiatr Genet* 20:113–117.
- Miller JE, Spiteri E, Condro MC, Dosumu-Johnson RT, Geschwind DH, White SA. 2008. Birdsong decreases protein levels of FoxP2, a molecule required for human speech. *J Neurophysiol* 100:2015–2025.
- Montagnese CM, Krebs JR, Meyer G. 1996. The dorsomedial and dorsolateral forebrain of the zebra finch, *Taeniopygia guttata*: a Golgi study. *Cell Tissue Res* 283:263–282.

- Newbury DF, Paracchini S, Scerri TS, Winchester L, Addis L, Richardson AJ, Walter J, Stein JF, Talcott JB, Monaco AP. 2011. Investigation of dyslexia and SLI risk variants in reading- and language-impaired subjects. *Behav Genet* 41:90–104.
- Nixdorf-Bergweiler BE. 1996. Divergent and parallel development in volume sizes of telencephalic song nuclei in male and female zebra finches. *J Comp Neurol* 375:445–456.
- Nottebohm F, Stokes TM, Leonard CM. 1976. Central control of song in the canary, *Serinus canarius*. *J Comp Neurol* 165:457–486.
- Ovsepian SV, Steuber V, Le Berre M, O'Hara L, O'Leary VB, Dolly JO. 2013. A defined heteromeric KV1 channel stabilizes the intrinsic pacemaking and regulates the output of deep cerebellar nuclear neurons to thalamic targets. *J Physiol (Lond)* 591:1771–1791.
- Panaïtof SC, Abrahams BS, Dong H, Geschwind DH, White SA. 2010. Language-related *Cntnap2* gene is differentially expressed in sexually dimorphic song nuclei essential for vocal learning in songbirds. *J Comp Neurol* 518:1995–2018.
- Pariani MJ, Spencer A, Graham JM, Rimoin DL. 2009. A 785kb deletion of 3p14.1p13, including the *FOXP1* gene, associated with speech delay, contractures, hypertonía and blepharophimosis. *Eur J Med Genet* 52:123–127.
- Peñagarikano O, Abrahams BS, Herman EI, Winden KD, Gdalyahu A, Dong H, Sonnenblick LI, Gruver R, Almajano J, Bragin A, Golshani P, Trachtenberg JT, Peles E, Geschwind DH. 2011. Absence of *CNTNAP2* leads to epilepsy, neuronal migration abnormalities, and core autism-related deficits. *Cell* 147:235–246.
- Peter B, Raskind WH, Matsushita M, Lisowski M, Vu T, Berninger VW, Wijsman EM, Brkanac Z. 2011. Replication of *CNTNAP2* association with nonword repetition and support for *FOXP2* association with timed reading and motor activities in a dyslexia family sample. *J Neurodev Disord* 3:39–49.
- Poliak S, Gollan L, Martínez R, Custer A, Einheber S, Salzer JL, Trimmer JS, Shrager P, Peles E. 1999. *Caspr2*, a new member of the neurexin superfamily, is localized at the juxtaparanodes of myelinated axons and associates with K⁺ channels. *Neuron* 24:1037–1047.
- Poliak S, Gollan L, Salomon D, Berglund EO, Ohara R, Ranscht B, Peles E. 2001. Localization of *Caspr2* in myelinated nerves depends on axon-glia interactions and the generation of barriers along the axon. *J Neurosci* 21:7568–7575.
- Poliak S, Salomon D, Elhanany H, Sabanay H, Kiernan B, Pevny L, Stewart CL, Xu X, Chiu S-Y, Shrager P, Furley AJ, Peles E. 2003. Juxtaparanodal clustering of Shaker-like K⁺ channels in myelinated axons depends on *Caspr2* and *TAG-1*. *J Cell Biol* 162:1149–1160.
- Price PH. 1979. Developmental determinants of structure in zebra finch song. *J Comp Physiol Psych* 93:260–277.
- Ramón y Cajal S. 1911. Le lobe optique des vertébrés inférieurs, toit optique des oiseaux. In: *Histologie du système nerveux de l'homme et des vertébrés*. Ramón y Cajal, ed. Paris: Maloine.
- Rasband WS. 1997–2012. ImageJ. U.S. National Institutes of Health, Bethesda, MD. <http://imagej.nih.gov/ij/>
- Reiner A, Perkel DJ, Bruce LL, Butler AB, Csillag A, Kuenzel W, Medina L, Paxinos G, Shimizu T, Striedter G, Wild M, Ball GF, Durand S, Güntürkün O, Lee DW, Mello CV, Powers A, White SA, Hough G, Kubikova L, Smulders TV, Wada K, Dugas-Ford J, Husband S, Yamamoto K, Yu J, Siang C, Jarvis ED. 2004. Revised nomenclature for avian telencephalon and some related brainstem nuclei. *J Comp Neurol* 473:377–414.
- Roberts TF, Wild JM, Kubke MF, Mooney R. 2007. Homogeneity of intrinsic properties of sexually dimorphic vocal motoneurons in male and female zebra finches. *J Comp Neurol* 502:157–169.
- Scott BB, Lois C. 2007. Developmental origin and identity of song system neurons born during vocal learning in songbirds. *J Comp Neurol* 502:202–214.
- Scott-Van Zeeland AA, Abrahams BS, Alvarez-Retuerto AI, Sonnenblick LI, Rudie JD, Ghahremani D, Mumford JA, Poldrack RA, Dapretto M, Geschwind DH, Bookheimer SY. 2010. Altered functional connectivity in frontal lobe circuits is associated with variation in the autism risk gene *CNTNAP2*. *Sci Transl Med* 2:56ra80.
- Simonyan K, Horwitz B, Jarvis ED. 2012. Dopamine regulation of human speech and bird song: a critical review. *Brain Lang* 122:142–150.
- Spiro JE, Dalva MB, Mooney R. 1999. Long-range inhibition within the zebra finch song nucleus RA can coordinate the firing of multiple projection neurons. *J Neurophysiol* 81:3007–3020.
- Stoeger AS, Mietchen D, Oh S, de Silva S, Herbst CT, Kwon S, Fitch WT. 2012. An asian elephant imitates human speech. *Curr Biol* 22:2144–2148.
- Strauss KA, Puffenberger EG, Huentelman MJ, Gottlieb S, Dobrin SE, Parod JM, Stephan DA, Morton DH. 2006. Recessive symptomatic focal epilepsy and mutant contactin-associated protein-like 2. *N Engl J Med* 354:1370–1377.
- Stroud JC, Wu Y, Bates DL, Han A, Nowick K, Paabo S, Tong H, Chen L. 2006. Structure of the forkhead domain of *FOXP2* bound to DNA. *Structure* 14:159–166.
- Südhof TC. 2008. Neuroligins and neurexins link synaptic function to cognitive disease. *Nature* 455:903–911.
- Teramitsu I, White SA. 2006. *FoxP2* regulation during undirected singing in adult songbirds. *J Neurosci* 26:7390–7394.
- Teramitsu I, Kudo LC, London SE, Geschwind DH, White SA. 2004. Parallel *FoxP1* and *FoxP2* expression in songbird and human brain predicts functional interaction. *J Neurosci* 24:3152–3163.
- Vernes SC, Newbury DF, Abrahams BS, Winchester L, Nicod J, Groszer M, Alarcón M, Oliver PL, Davies KE, Geschwind DH, Monaco AP, Fisher SE. 2008. A functional genetic link between distinct developmental language disorders. *N Engl J Med* 359:2337–2345.
- Vicario DS. 1991. Organization of the zebra finch song control system: II. Functional organization of outputs from nucleus *Robustus archistriatalis*. *J Comp Neurol* 309:486–494.
- White SA. 2010. Genes and vocal learning. *Brain Lang* 115:21–28.
- Whitehouse AJO, Bishop DVM, Ang QW, Pennell CE, Fisher SE. 2011. *CNTNAP2* variants affect early language development in the general population. *Genes Brain Behav* 10:451–456.
- Whitney O, Johnson F. 2005. Motor-induced transcription but sensory-regulated translation of *ZENK* in socially interactive songbirds. *J Neurobiol* 65:251–259.
- Wild JM, Williams MN, Suthers RA. 2001. Parvalbumin-positive projection neurons characterise the vocal premotor pathway in male, but not female, zebra finches. *Brain Res* 917:235–252.
- Wild JM, Williams MN, Howie GJ, Mooney R. 2005. Calcium-binding proteins define interneurons in HVC of the zebra finch (*Taeniopygia guttata*). *J Comp Neurol* 483:76–90.
- Wild JM, Kubke MF, Mooney R. 2009. Avian nucleus retroambigualis: cell types and projections to other respiratory-vocal nuclei in the brain of the zebra finch (*Taeniopygia guttata*). *J Comp Neurol* 512:768–783.
- Xu X, Coats JK, Yang CF, Wang A, Ahmed OM, Alvarado M, Izumi T, Shah NM. 2012. Modular genetic control of sexually dimorphic behaviors. *Cell* 148:596–607.